

Adaptive Mesh Simulations of Pellet Injection in Tokamaks

Ravi Samtaney

Computational Plasma Physics Group
Princeton Plasma Physics Laboratory
Princeton University

SIAM Annual Conference

July 10-14 2006, Boston, MA



Acknowledgement: DOE SciDAC Program

Collaborators

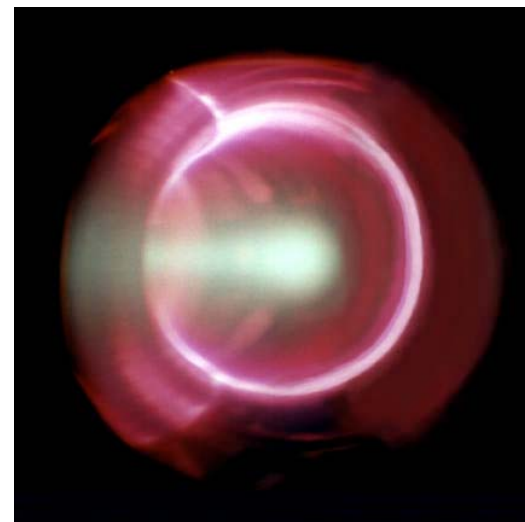
- P. Colella and Applied Numerical Algorithms Group (LBNL)
- S. C. Jardin (PPPL)
- P. Parks (GA)
- D. Reynolds (UCSD)
- C. Woodward (LLNL)
- Funded through the TOPS, CEMM and APDEC SciDAC Centers. RS supported by US DOE Contract No. DE-AC020-76-CH03073

Outline

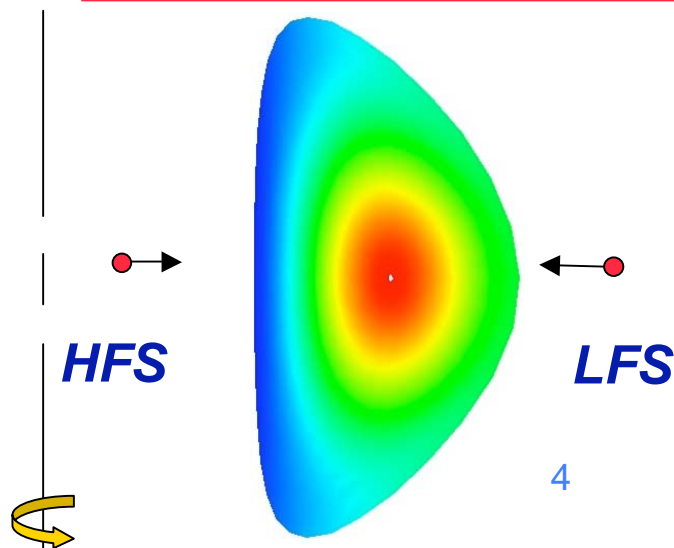
- Introduction and motivation
- Description of physical phenomenon
 - *Spatial and temporal scales*
- Equations and models
- Adaptive mesh refinement (AMR) for shaped plasma in flux-surface coordinates
- Results
 - *HFS vs. LFS Pellet injection*
- Newton-Krylov fully implicit method
- Future directions and conclusion

Pellet Injection & Edge Localized Modes

- Motivation
 - Injection of frozen hydrogen pellets is a viable method of fueling a tokamak
 - Presently there is no satisfactory simulation or comprehensive predictive model for pellet injection (esp. for ITER)
 - H-mode operation of ITER will be accompanied by edge localized modes (ELMS) (ITER Physics Experts Group, Nucl. Fusion 1999)
 - Pellet injection related to ELMS (Gohill et al. PRL, 2001; Lang et al. Nucl. Fusion 2000)
- Objectives
 - Develop a comprehensive simulation capability for pellet injection and ELMS in tokamaks (esp. ITER) with modern technologies such as adaptive mesh refinement for spatial resolution and fully implicit Newton-Krylov approach for temporal stiffness



Pellet injection in TFTR



Physical Processes: Description

- Non-local electron transport along field lines rapidly heats the pellet cloud (τ_e).
 - Frozen pellet encounters hot plasma and ablates rapidly
 - Neutral gas surrounding the solid pellet is ionized
 - Ionized, but cool plasma, continues to get heated by electrons
 - A high β “plasmoid” is created
- Ionized plasmoid expands
 - Fast magnetosonic time scale τ_f
- Pellet mass moves across flux surfaces τ_a .
 - So-called “anomalous” transport across flux surfaces is accompanied by reconnection
- Pellet cloud expands along field lines τ_c .
 - Pellet mass distribution continues along field lines until pressure equilibration
- Pellet lifetime τ_p

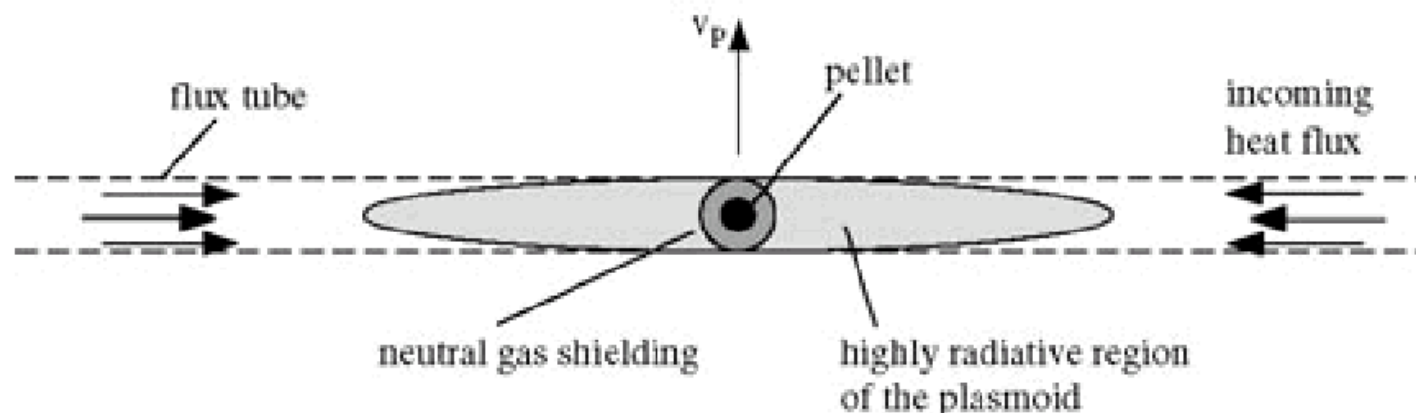


Figure from Müller et al., Nuclear Fusion 42 (2002)

Scales and Resolution Requirements

- Time Scales $\tau_e < \tau_f < \tau_a < \tau_c < \tau_p$
- Spatial scales: Pellet radius $r_p \ll$ Device size $L \sim O(10^{-3})$
- Presence of magnetic reconnection further complicates things
 - *Thickness of resistive layer scales with $\sim \eta^{1/2}$*
 - *Time scale for reconnection is $\sim \eta^{-1/2}$*
- Pellet cloud density $\sim O(10^4)$ times ambient plasma density
- Electron heat flux is non-local
- Large pressure and density gradients in the vicinity of cloud
- Pellet lifetime $\sim O(10^{-3})$ s \rightarrow long time integrations

Resolution estimates

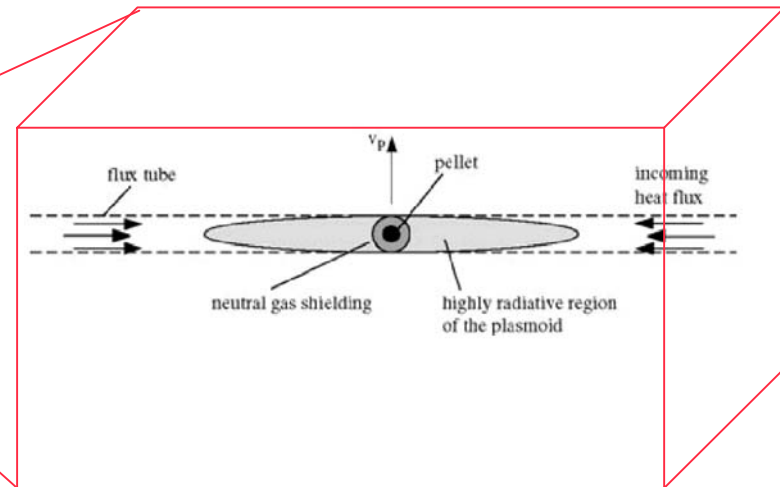
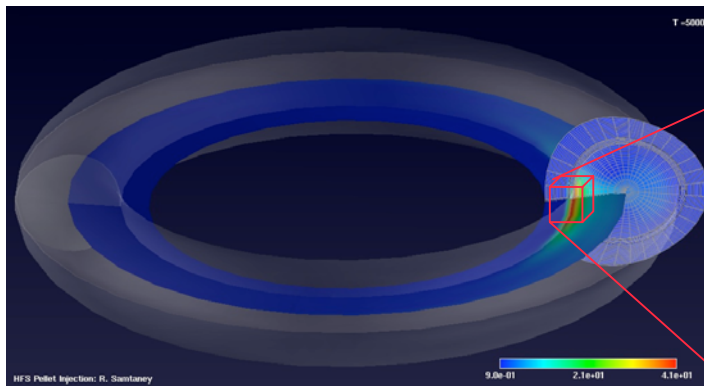
Tokamak	Major Radius	N	N_{steps}	Spacetime Points
CDXU (Small)	0.3	2×10^7	2×10^5	4×10^{12}
DIID (Medium)	1.75	3.3×10^9	7×10^6	2.3×10^{17}
ITER (Large)	6.2	1.5×10^{11}	9×10^7	1.4×10^{19}

Related Work - Local vs. Global Simulations

- Earliest ablation model by Parks (Phys. Fluids 1978)
 - Detailed multi-phase calculations in 2D of pellet ablation (MacAulay, PhD thesis, Princeton Univ 1993, Nuclear Fusion 1994)
 - Detailed 2D Simulations of pellet ablation by Ishizaki, Parks et al. (Phys. Plasmas 2004)
 - *Included atomic processes – ablation, dissociation, ionization, pellet fluidization and distortion; semi-analytical model for electron heat flux from background plasma*
 - In above studies, the domain of investigation was restricted to only a few cm around the pellet
 - *Furthermore, in these studies the magnetic field was static*
-
- 3D Simulations by Strauss and Park (Phys. Plasmas, 1998)
 - *Solve an initial value problem. Initial condition consisted of a density “blob” to mimic a fully ablated pellet cloud which, compared with device scales, was relatively large due to resolution restrictions*
 - *No motion of pellet modeled*
 - 3D Adaptive Mesh Simulation of pellet injection by Samtaney et al. (Comput. Phys. Comm, 2004)

Current Work

- Combine global MHD simulations in a tokamak geometry with detailed local physics including ablation, ionization and electron heating in the neighborhood of the pellet



- AMR techniques to mitigate the complexity of the multiple scales in the problem
- Newton-Krylov approach for wide range of temporal scales

Mathematical Model

- Single fluid resistive MHD equations in conservation form

$$\frac{\partial U}{\partial t} + \underbrace{\left(\frac{1}{R} \frac{\partial RF}{\partial R} + \frac{\partial H}{\partial z} + \frac{1}{R} \frac{\partial G}{\partial \phi} \right)}_{\text{Hyperbolic terms}} = S + \underbrace{\left(\frac{1}{R} \frac{\partial RF_D}{\partial R} + \frac{\partial H_D}{\partial z} + \frac{1}{R} \frac{\partial G_D}{\partial \phi} \right)}_{\text{Diffusive terms}} + S_D + S_{\text{pellet}}$$

Hyperbolic terms

Diffusive terms

Density: Ablation
Energy :Electron heat flux

$$U = \{\rho, \rho u_R, \rho u_\phi, \rho u_Z, B_R, B_\phi, B_Z, e\}^T$$

$$F \equiv F(U) = \begin{Bmatrix} \rho u_R \\ \rho u_R^2 + p_t - B_R^2 \\ \rho u_R u_\phi - B_R B_\phi \\ \rho u_R u_Z - B_R B_Z \\ 0 \\ u_R B_Z - u_Z B_R \\ u_R B_\phi - u_\phi B_R \\ (e + p_t) u_R - (B_l u_l) B_R \end{Bmatrix}, \quad H \equiv H(U) = \begin{Bmatrix} \rho u_Z \\ \rho u_R u_Z - B_R B_Z \\ \rho u_Z u_\phi - B_Z B_\phi \\ \rho u_Z^2 + p_t - B_Z^2 \\ u_Z B_R - u_R B_Z \\ 0 \\ u_Z B_\phi - u_\phi B_Z \\ (e + p_t) u_Z - (B_k u_k) B_Z \end{Bmatrix},$$

$$G \equiv G(U) = \begin{Bmatrix} \rho u_\phi \\ \rho u_R u_\phi - B_R B_\phi \\ \rho u_\phi^2 + p_t - B_\phi^2 \\ \rho u_Z u_\phi - B_Z B_\phi \\ u_\phi B_R - u_R B_\phi \\ u_\phi B_Z - u_Z B_\phi \\ 0 \\ (e + p_t) u_\phi - (B_k u_k) B_\phi \end{Bmatrix}, \quad S(U) = -\frac{1}{R} \begin{Bmatrix} 0 \\ B_\phi^2 - \rho u_\phi^2 - p_t \\ \rho u_R u_\phi - B_R B_\phi \\ 0 \\ 0 \\ 0 \\ 0 \\ u_\phi B_R - u_R B_\phi \end{Bmatrix}$$

- Additional constraint $\nabla \cdot \mathbf{B} = 0$

Ablation Model

- Mass source is given using the ablation model by Parks and Turnbull (Phy. Plasmas 1978) and Kuteev (Nuclear Fusion 1995)

$$\frac{dN}{dt} = -4\pi r_p^2 \frac{dr_p}{dt} 2n_m = 1.12 \times 10^{16} n_e^{0.333} T_e^{1.64} r_p^{1.33} M_i^{-0.333}$$

– Above equation uses cgs units

- Abalation occurs on the pellet surface

$$S_n = \dot{N} \delta(x - x_p)$$

- Regularized as a truncated Gaussian of width $10 r_p$
- Pellet shape is spherical for all t
- Pellet trajectory is specified as either HFS or LFS
- Monte Carlo integration to determine average source in each finite volume

Electron Heat Flux Model

- Semi-analytical Model by Parks et al. (Phys. Plasmas 2000)
 - Assumes Maxwellian electrons and neglects pitch angle scattering

$$-\nabla \cdot q_e = \frac{q_\infty n}{\tau_\infty} [g(u_+) + g(u_-)]$$

$$q_\infty = \sqrt{\frac{2}{\pi m_e}} n_{e\infty} (k T_{e\infty})^{\frac{3}{2}} \quad \tau_\infty = \frac{T_{e\infty}^2}{8\pi e^4 \log \Omega} \quad g(u) = u^{\frac{1}{2}} K_1(u^{\frac{1}{2}})/4$$

$$u_\pm = \frac{\tau_\pm}{\tau_\infty} \quad \tau_\pm = \pm \int_{\mp\infty}^{\mathbf{x}} n(s) ds$$

- Solve for opacities as a “steady-state” solution to an advection-reaction equation

- Solve by using an upwind method

- Advection velocity is \mathbf{b}

$$\frac{d\tau}{ds} = n(\mathbf{x}) \quad \hat{\mathbf{b}} \cdot \nabla \tau = n(\mathbf{x})$$

$$\frac{d\tau}{d\zeta} + \hat{\mathbf{b}} \cdot \nabla \tau = n(\mathbf{x})$$

- Ansatz for energy conservation

- Sink term on flux surface outside cloud

$$-\nabla \cdot q_e = \frac{1}{V_\psi - V_{cloud,\psi}} \int_{cloud,\psi} \nabla \cdot q_e$$

Curvilinear coordinates for shaped plasma

- Adopt a flux-tube coordinate system (flux surfaces ψ are determined from a separate equilibrium calculation)
 - $R \equiv R(\xi, \eta)$, and $Z \equiv Z(\xi, \eta)$
 - $\xi \equiv \xi(R, Z)$, and $\eta \equiv \eta(R, Z)$
 - Flux surfaces: $\psi = \psi_0 \xi$
 - ϕ coordinate is retained as before

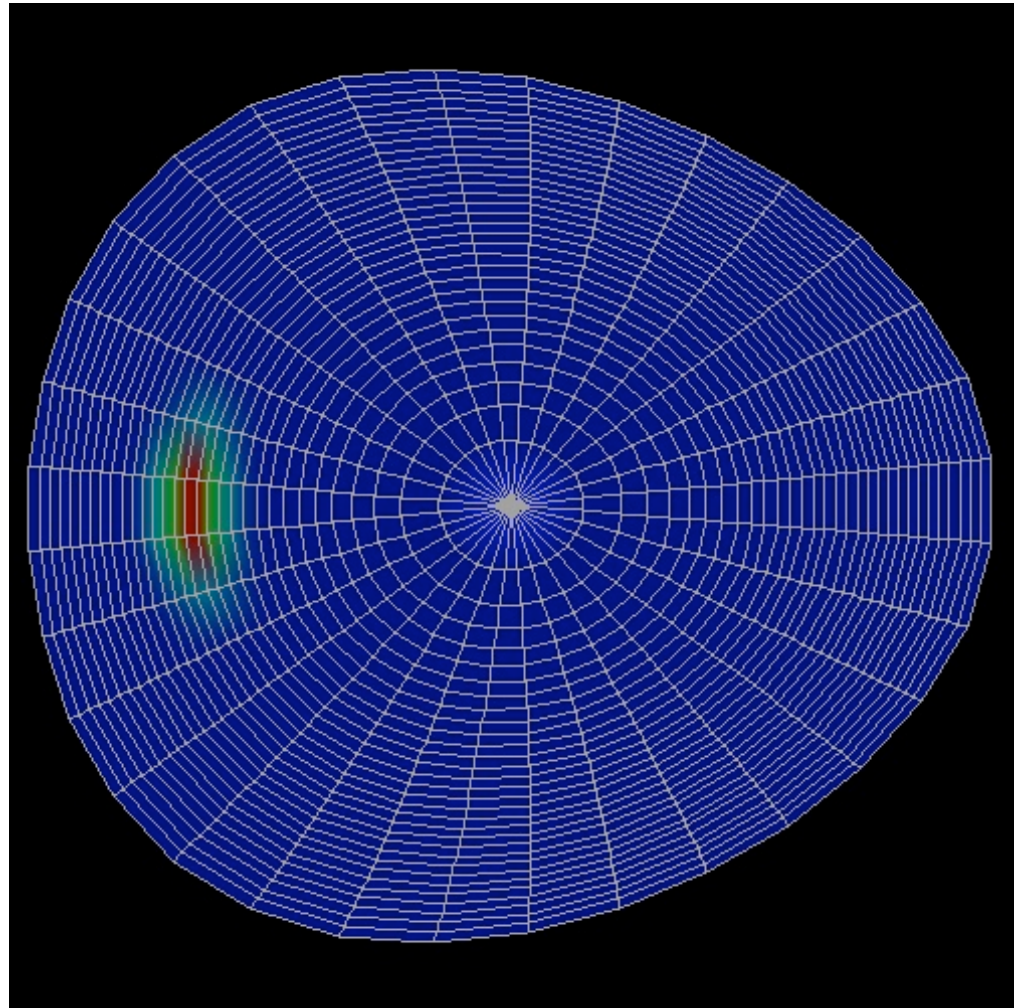
- Equations in transformed coordinates

$$\frac{\partial UJ}{\partial t} + \frac{1}{R} \frac{\partial R\tilde{F}}{\partial \xi} + \frac{1}{R} \frac{\partial R\tilde{H}}{\partial \eta} + \frac{1}{R} \frac{\partial \tilde{G}}{\partial \phi} = \tilde{S}$$

$$\tilde{F} = J(\xi_R F + \xi_z H) = z_\eta F - R_\eta H,$$

$$\tilde{H} = J(\eta_R F + \eta_z H) = -z_\xi F + R_\xi H,$$

$$\tilde{G} = JG, \quad \tilde{S} = JS.$$

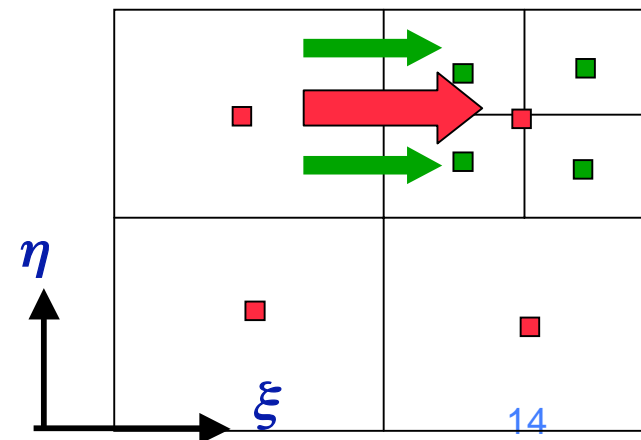


Numerical method

- Finite volume approach
- Explicit second order or third order TVD Runge-Kutta time stepping
- The hyperbolic fluxes are evaluated using upwinding methods
 - *seven-wave Riemann solver*: $F \equiv F(U_L, U_R) = \frac{1}{2}(F(U_L) + F(U_R)) - \sum_k \alpha_k |\lambda_k| r_k$ where $\alpha_k = I_k (U_R - U_L)$
 - *Harten-Lee-vanLeer (HLL) Method* (SIAM Review 1983)
 $F \equiv F(U_L, U_R) = \lambda_{\min} F(U_L) + \lambda_{\max} F(U_R) + \lambda_{\min} \lambda_{\max} (U_R - U_L) / (\lambda_{\max} - \lambda_{\min})$
- Diffusive fluxes computed using standard second order central differences
- The solenoidal condition on \mathbf{B}
 - *imposed using the Central Difference version of Constrained Transport* (Toth JCP 161, 2000)
 - *Including the non-conservative source term in the equation to advect $\nabla \cdot \mathbf{B}$ errors* (Powell et al., JCP 1999)
 - *By projection at $n+1/2$ time step* (Samtaney et al., SciDAC 2005)
 - $\nabla \cdot \mathbf{B} \neq 0$ on coarse mesh cells adjacent to coarse-fine interfaces
- **Initial Conditions:** Express $\mathbf{B} = 1/R(\phi \times \nabla \psi + g(\psi) \phi) \neq \text{fnc}(\phi)$.
Initial state is an MHD equilibrium obtained from a Grad-Shafranov solver.
- **Boundary Conditions:** Perfectly conducting for $\xi = \xi_0$, zero flux (due to zero area) at $\xi = \xi_i$, and periodic in η and ϕ .

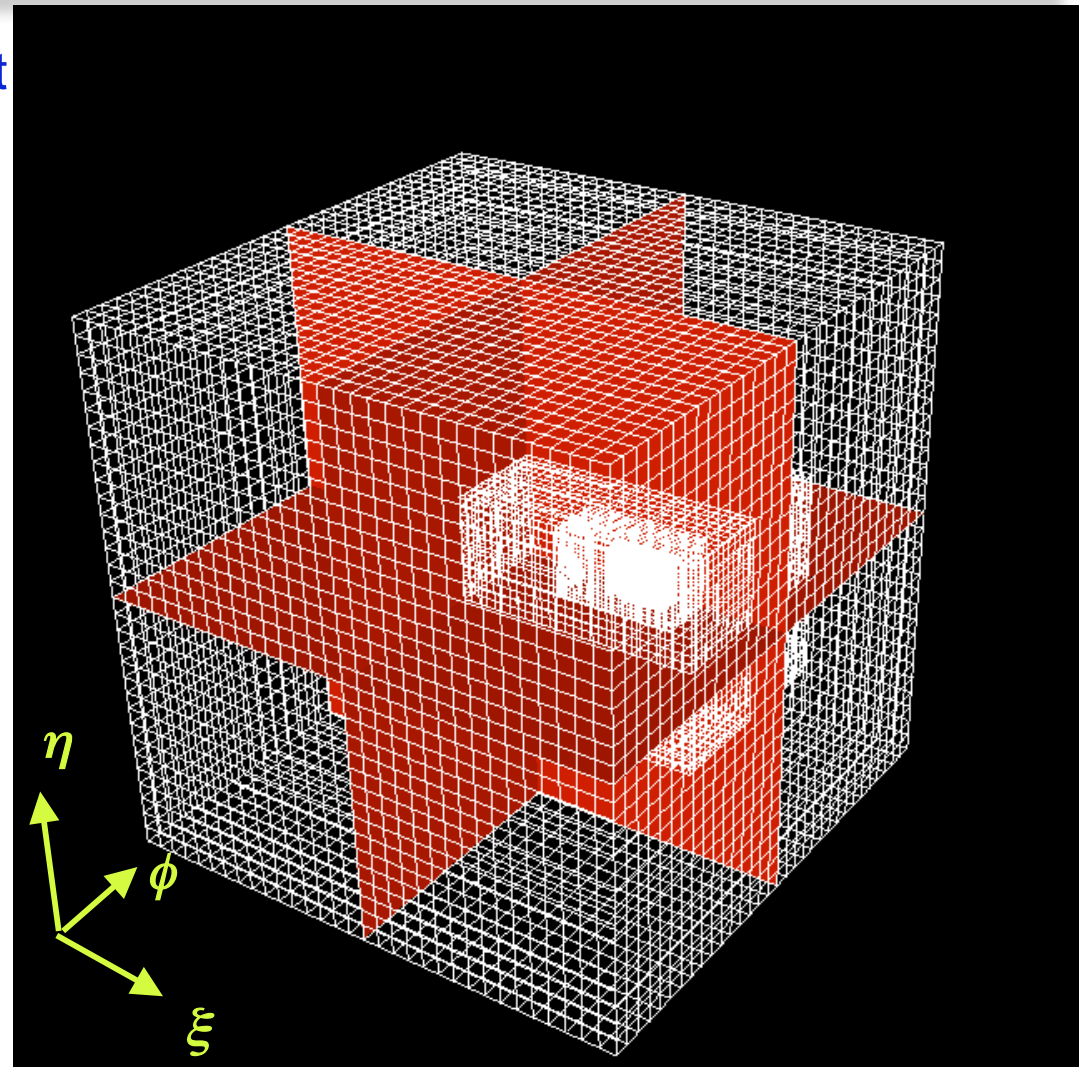
Adaptive Mesh Refinement with Chombo

- **Chombo** is a collection of C++ libraries for implementing block-structured adaptive mesh refinement (AMR) finite difference calculations
(<http://www.seesar.lbl.gov/ANAG/chombo>)
 - (*Chombo is an AMR developer's toolkit*)
- **Adaptivity in both space and time**
- Mesh generation: necessary to ensure volume preservation and areas of faces upon refinement
- Flux-refluxing step at end of time step ensures conservation

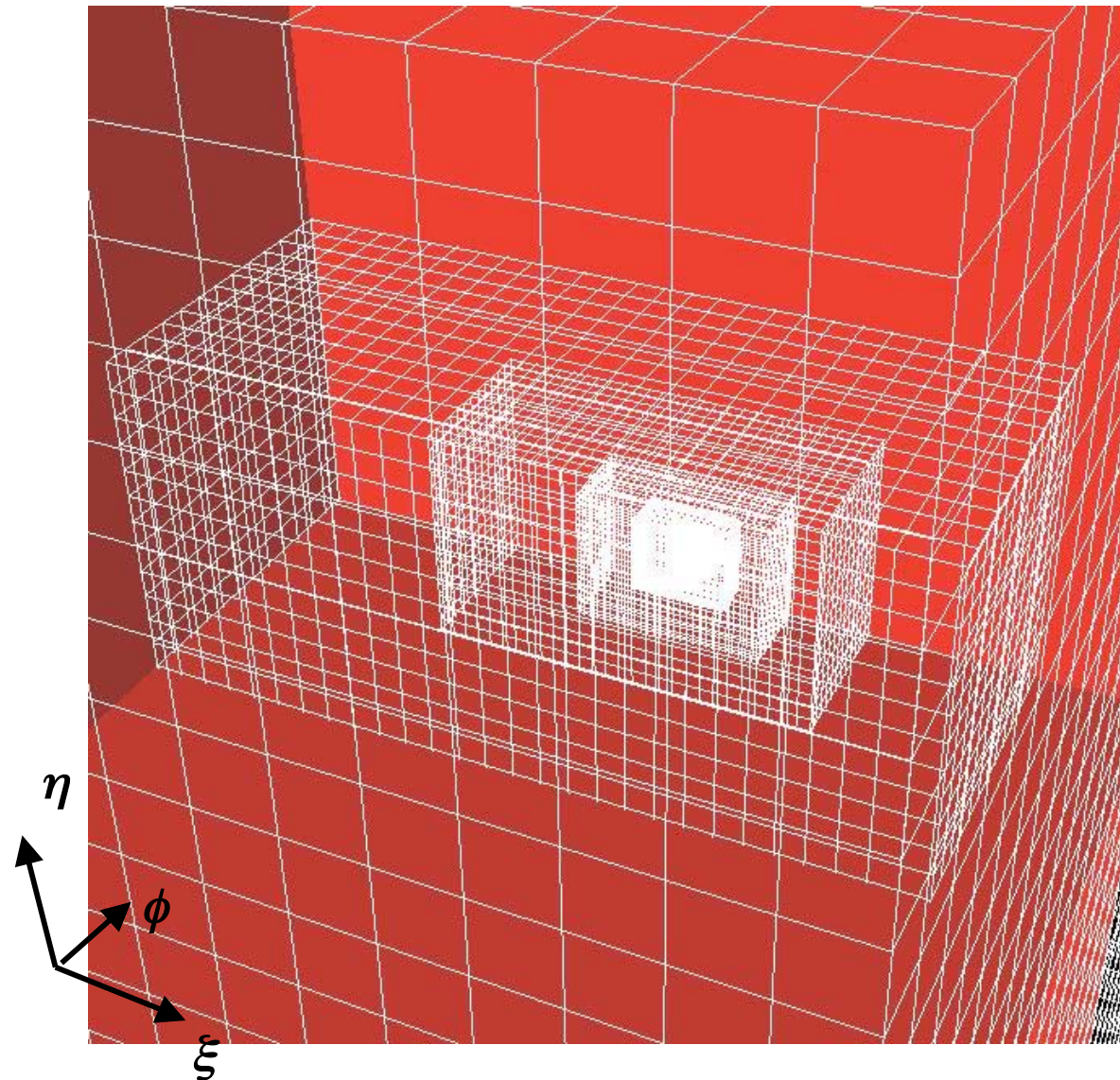


Pellet Injection: AMR

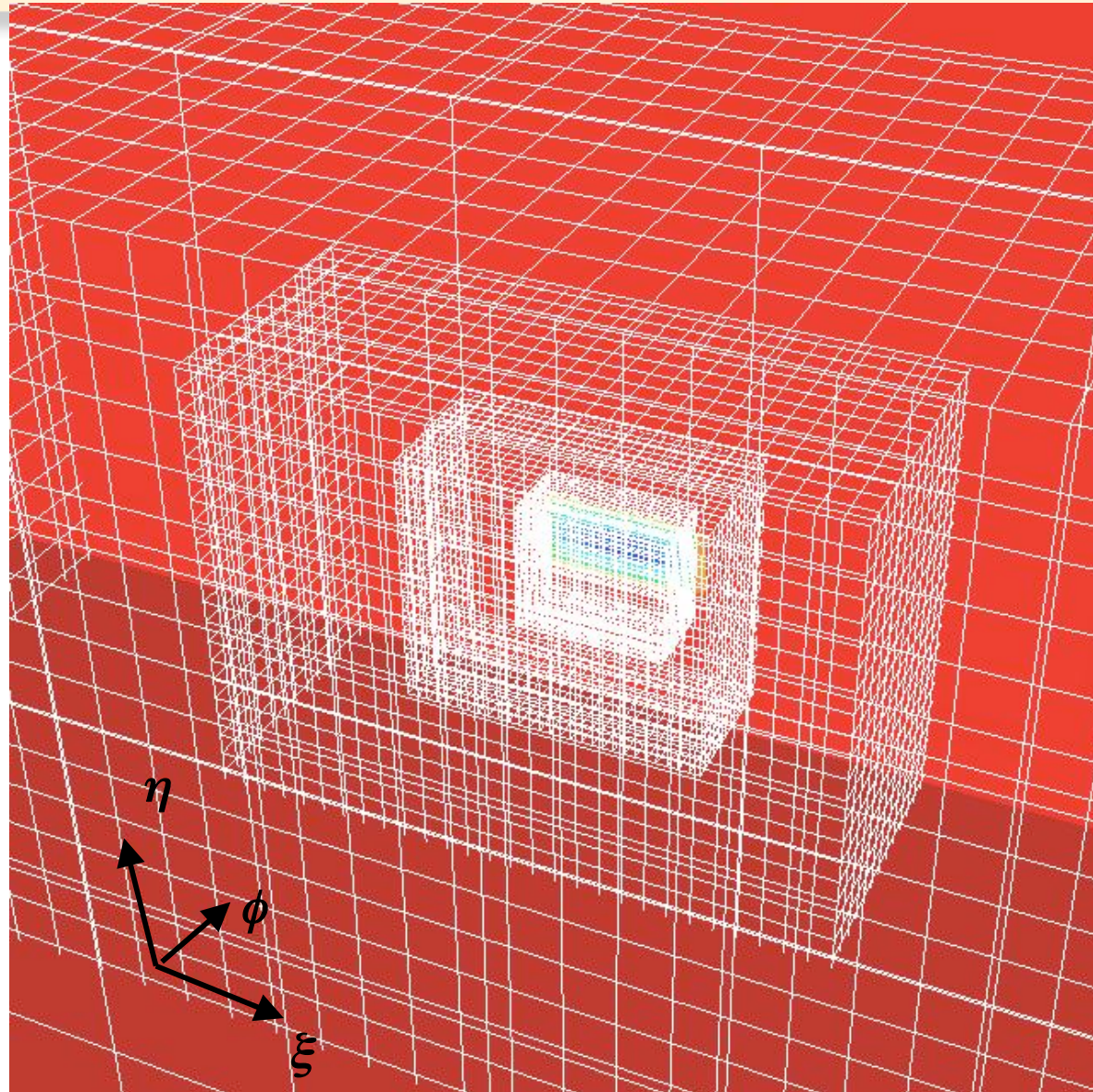
- Meshes clustered around pellet
- Computational space mesh structure shown on right
- Mesh stats
 - 32^3 – base mesh with 5 levels, and refinement factor 2
 - Effective resolution: 1024^3
 - Total number of finite volume cells: 113408
 - Finest mesh covers 0.015 % of the total volume
 - Time adaptivity:
 $1 (\Delta t)_{\text{base}} = 32 (\Delta t)_{\text{finest}}$



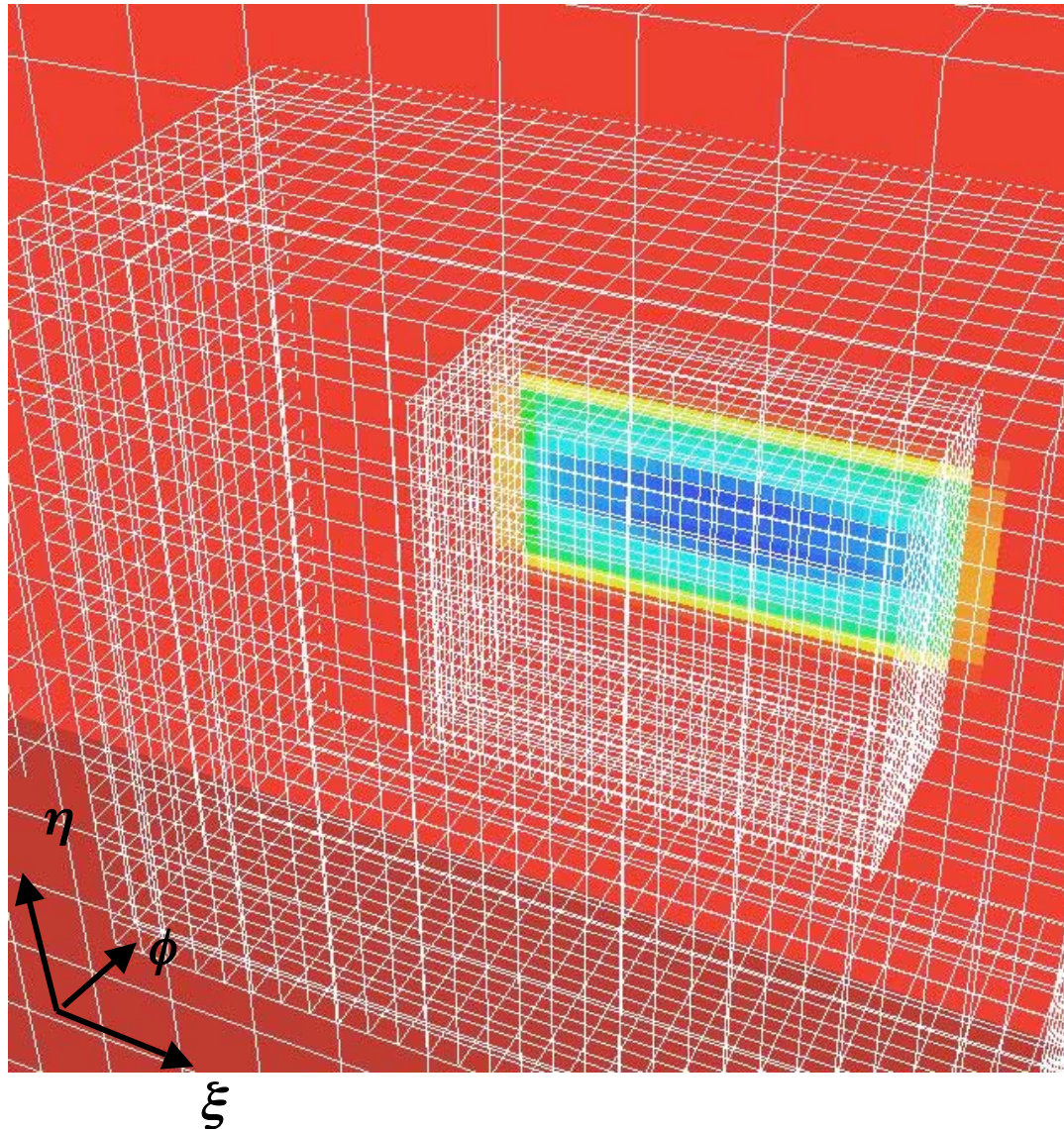
Pellet Injection: Zoom into Pellet Region



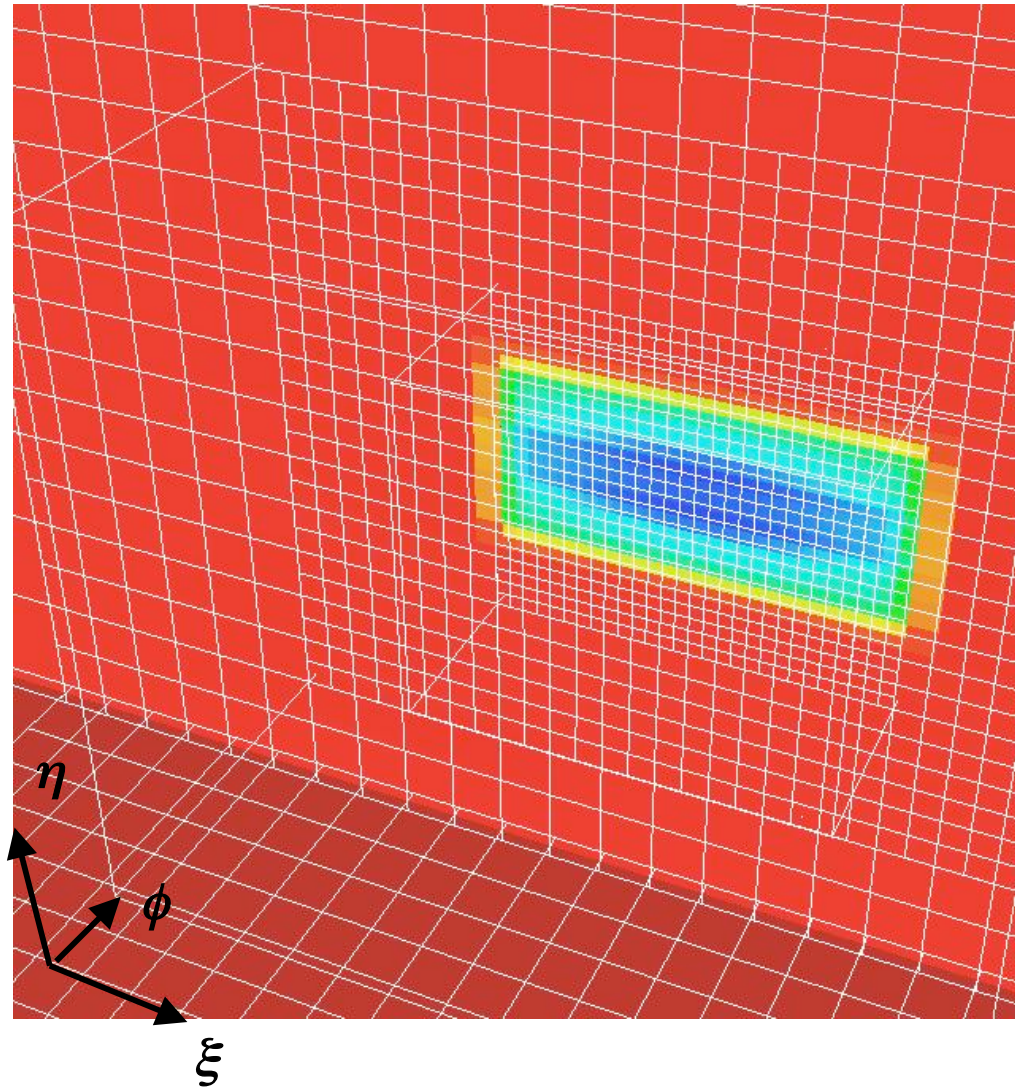
Pellet Injection: Zoom in



Pellet Injection: Pellet in Finest Mesh

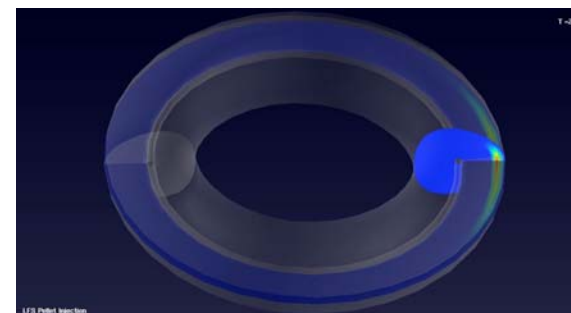
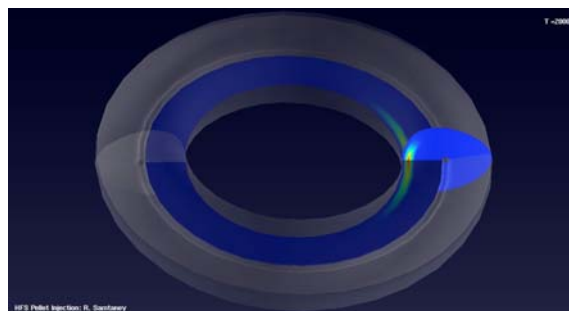


Pellet Injection: Pellet Cloud Density

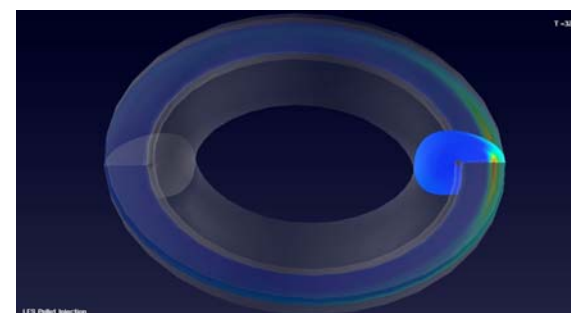
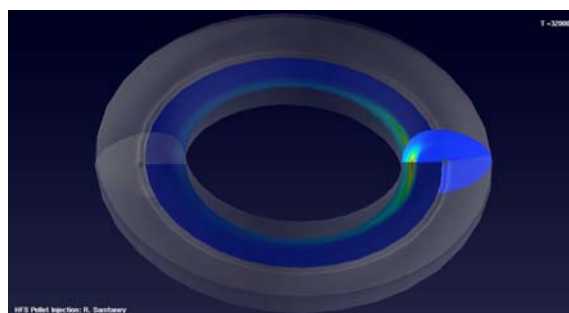


Results - HFS vs. LFS

$B_T = 0.375T$
 $n_0 = 1.5 \times 10^{19}/m^3$
 $T_{e\infty} = 1.3Kev$
 $\beta = 0.05$
 $R_0 = 1m, a = 0.3 m$
 Pellet: $r_p = 1mm,$
 $v_p = 1000m/s$

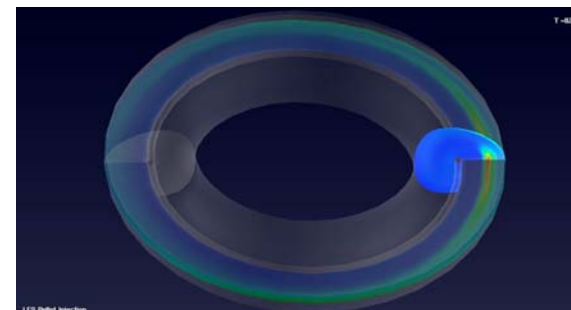
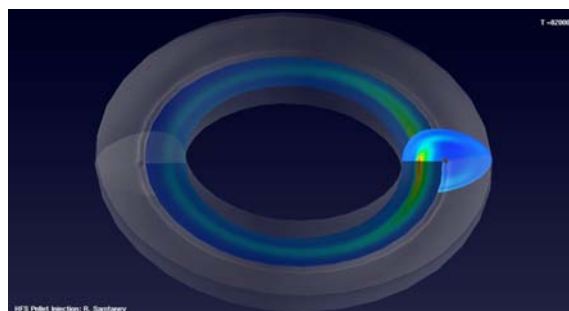


$t=7$



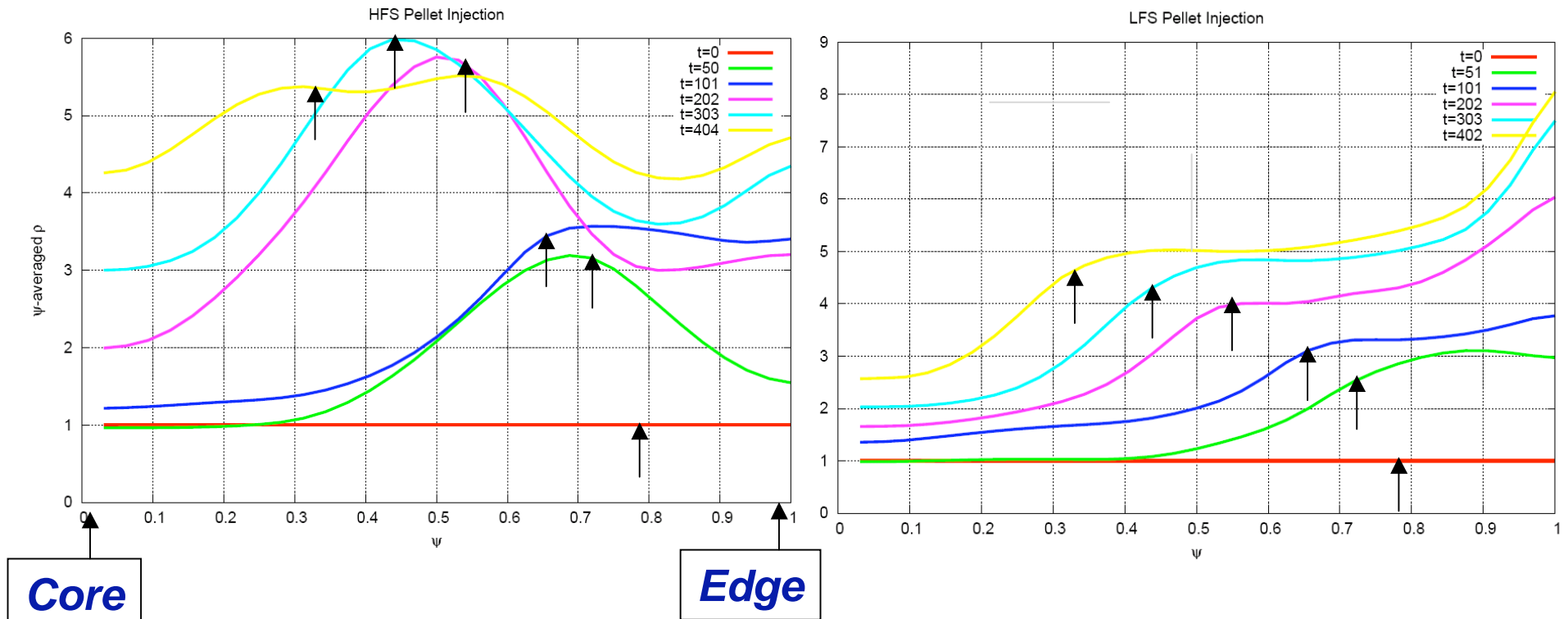
ρ

$t=100$



$t=256$

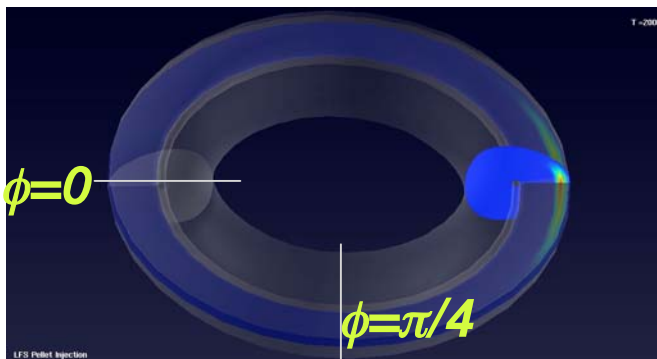
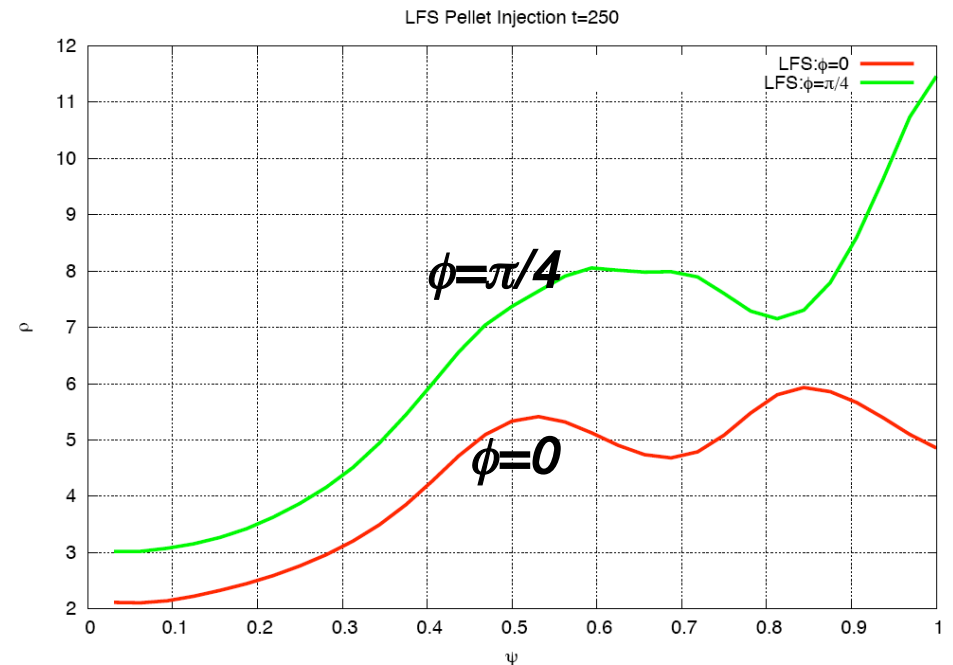
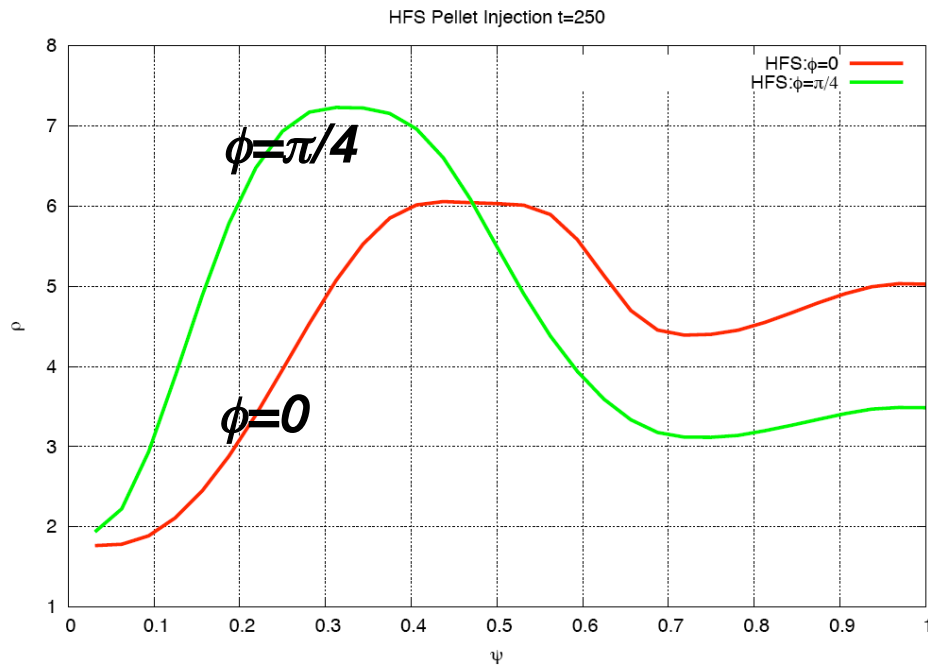
HFS vs. LFS - Average Density Profiles



HFS Pellet injection shows better core fueling than LFS

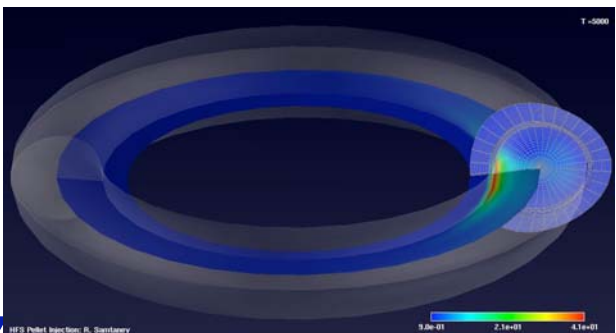
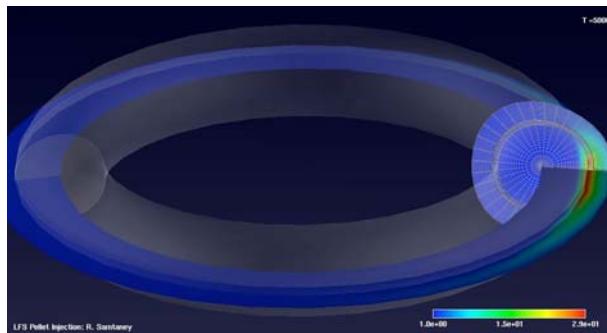
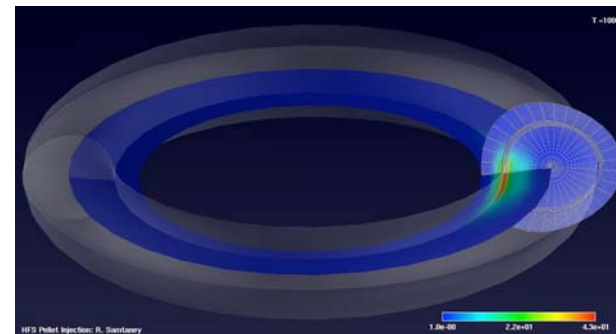
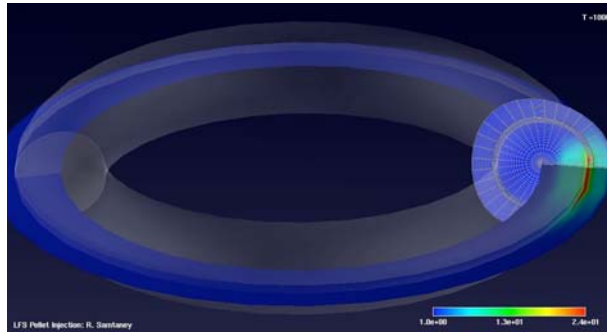
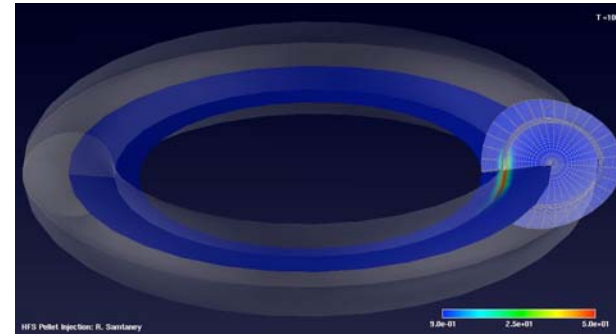
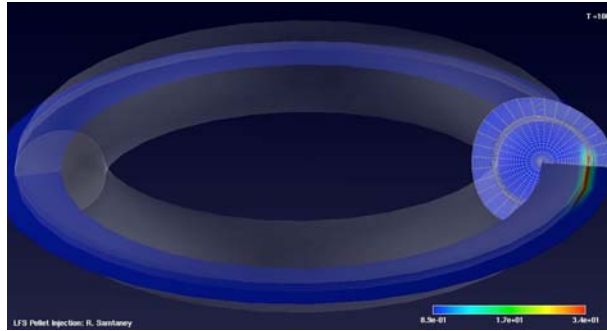
Arrows indicate average pellet location

HFS vs. LFS: Instantaneous Density Profiles



Radially outward shift in both cases indicates higher fueling effectiveness for HFS

Pellet Injection: LFS/HFS Launch



Density

JFNK Fully Implicit Approach for Resistive MHD

- Time step set using explicit CFL condition of fastest wave: $\Delta t_{\text{cfl}} \leq \frac{\Delta x}{\|v+c_f\|_1}$
- Pellet Injection: pellet radius $r_p = 0.3$ mm, injection velocity $v_p = 450$ m/s, fast magneto-acoustic speed $c_f \approx 10^6$ m/s:

– *To resolve pellet need $O(10^7)$ time steps*

- Longer time steps (implicit methods) are a practical necessity
- Fixed time step, two-level θ -scheme using a Jacobian-Free Newton-Krylov nonlinear solver [KINSOL]:

$$f(U^n) = U^n - U^{n-1} - \Delta t [\theta g(U^n) + (1-\theta)g(U^{n-1})], \quad g(U) = \nabla \cdot (F^p(U) - F^h(U))$$

– $\theta = 1 \Rightarrow$ *Backward Euler [$O(\Delta t)$]; $\theta = 0.5 \Rightarrow$ *Cranck-Nicholson [$O(\Delta t^2)$]**

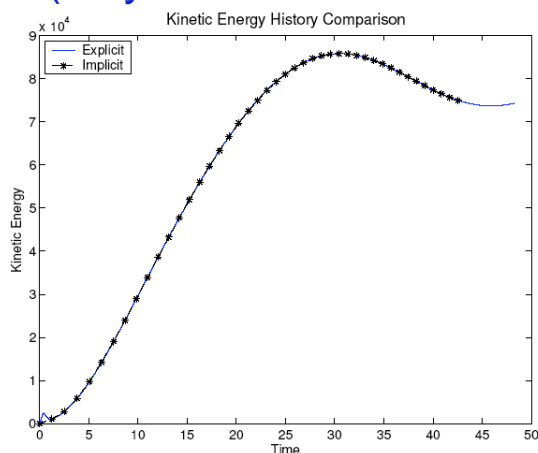
- Adaptive time step, adaptive order, BDF method for an up to 5th order accurate implicit scheme [CVODE]:

$$f(U^n) = U^n - \sum_{i=1:q} \alpha_{n,i} U^{n-i} - \Delta t_n \beta_{n,1} g(U^{n-1}) - \Delta t_n \beta_0 g(U^n)$$

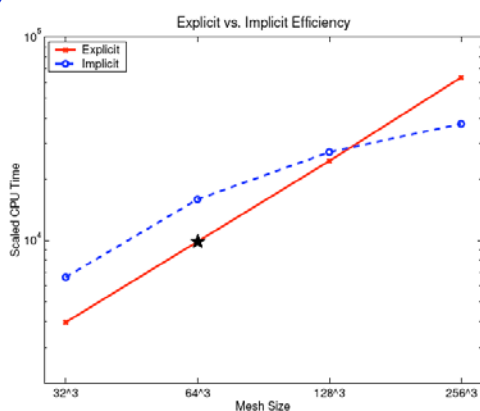
Time step size and order adaptively chosen based on heuristics balancing accuracy, nonlinear & linear convergence, stability

Pellet Injection - Implicit Simulations

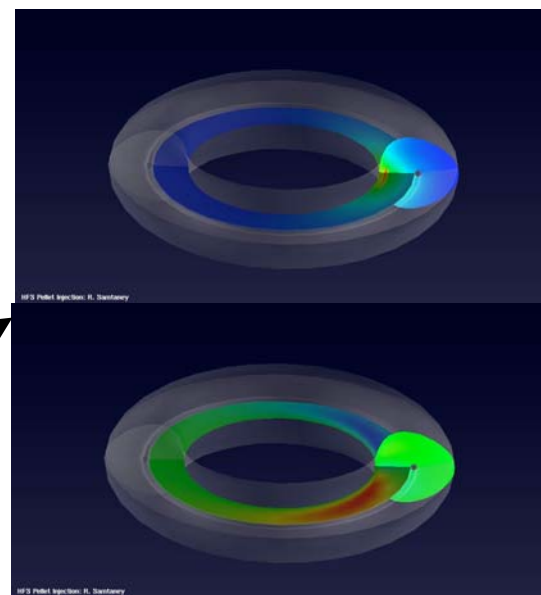
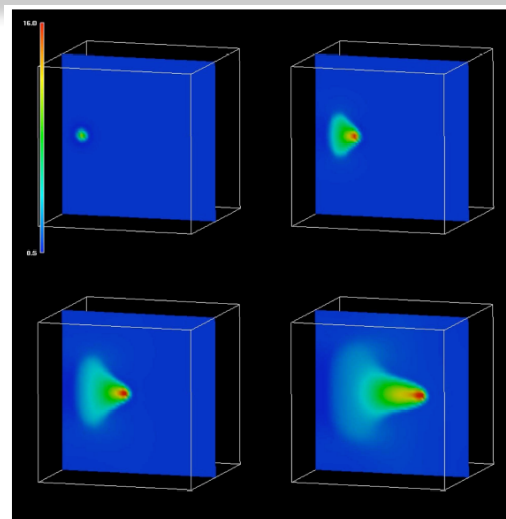
- Choose a model problem with a similar separation of time scales (Reynolds et al. JCP 2006)



Good agreement between explicit and implicit methods



Implicit (no preconditioners) overtakes explicit method as problem size gets larger.



Implicit simulations in a toroidal geometry. $\Delta t = 100 \Delta t_{\text{explicit}}$

Summary and Future Plan

- Preliminary results presented from an AMR MHD code
 - *Physics of non-local electron heat flux included*
 - *HFS vs. LFS pellet launches*
 - *HFS core fueling is more effective than LFS*
 - *Numerical method is upwind, conservative and preserves the solenoidal property of the magnetic field*
- AMR provides the resolution to simulate pellet injection in a tokamak with detailed local physics
- Preliminary results from a fully implicit Newton-Krylov method for pellet injection in tokamaks
- Future work
 - *Physics-based pre-conditioners for fully implicit JFNK method for mapped-grids and tokamak geometry.*
 - *Proposed work under SciDAC-2: Combine adaptive and fully implicit methods to manage the wide range of spatial and temporal scales*